KNOCKOUT REACTIONS

STUDY OF DIPOLE RESONANCE STRENGTH IN ^{12}C VIA THE REACTIONS ^{12}C$(\vec{p}, p'c)$

W.D. Anderson, L.C. Bland, D.S. Carman, G.M. Huber, B.C. Markham,
D.W. Miller, K. Murphy, B.A. Raue, P.Schwandt, J.A. Templon
Indiana University Cyclotron Facility, Bloomington, Indiana 47408

IUCF experiment E321 is an angular correlation study of the ^{12}C(p,p'c) reaction at T_p=155.8 MeV (where "c" represents any charged particle). The motivation for this experiment is to gain an improved understanding of the low–excitation ($E_x \leq$40 MeV) ^{12}C continuum excited by small momentum transfer (q$\leq$1.20 fm^{-1}) proton inelastic scattering. It is anticipated that in this (q,ω) domain, different spin/isospin components of the ΔL=1 particle–hole response will predominate. The angular correlation function of coincident charged–particle decays is expected to help identify the multipolarity of overlapping resonances in the intermediate state as well as distinguish resonance excitation from the non-resonant quasifree knockout "background" which plagues inclusive measurements.[1] The experiment was performed at three different proton scattering angles to aid the multipole decomposition. Data for the inclusive cross section and analyzing power for the ^{12}C(p,p') reaction were obtained simultaneously with the exclusive ^{12}C(p,p'c) data. Measurements were completed at three angles: $\theta_{p'}$=14.3, 19.0, and 24.0°.

The K600 spectrometer was utilized to detect inelastically scattered protons. The forward–angle limit for the spectrometer of 14.3° was imposed by the exit pipe necessary for transporting the beam to the external faraday cup. Coincident charged particles were detected in a coplanar geometry by an array of eight counter telescopes mounted in the 61 cm vacuum chamber. Four telescopes were placed on the left and right sides of the beam in 25° intervals covering the angular range from 0° to 180° for charged particle decays from ^{12}C* resonant states. Each telescope consisted of a 2.54 cm diameter, 0.01 cm thick (ΔE) silicon surface barrier detector and a 2.54 cm diameter, 0.5 cm thick (E) lithium-drifted silicon detector. The detectors were operated at 0° C to optimize their pulse–height resolution and to minimize radiation damage. Each detector pair was mounted in a 0.64 cm thick brass shielding enclosure that had a circular aperture viewing the target. The solid angle for all but the most forward telescope was 5 msr. Singles rates in the telescopes were less than 10 kHz for a luminosity of $\leq$6.8 × 10^{31} cm^{-2}s^{-1}. Particle identification was accomplished using either ΔE vs. E or time of flight vs. E correlations. Clean separation of all particle groups was achieved covering the dynamic range from the 1–MeV telescope detection threshold up to 25–MeV protons.

Event triggering was accomplished by forming the logical OR of the ΔE and E detectors of each telescope. The eightfold OR of the telescope triggers independently latched pulse–height and timing data for the detector array. The standard focal plane trigger (scintillator coincidence) was used to latch data from the vertical drift chambers and the scintillators. A sample of the singles data from the K600 focal plane and the detector array

was read out by the computer for the inclusive (p,p′) measurements and for monitoring purposes. A coincidence between any member of the detector array and the K600 focal plane triggered computer readout of all data. The resolving time of the overlap was long enough to permit direct measurements of accidental coincidences necessary for the offline analysis. CAMAC data was cleared by a hardware signal for noncoincident events.

An analysis of the (p,p′c) data has been completed including most of the essential corrections to the data. These corrections include calculating detection efficiencies of particle "c" accounting for detector thresholds, energy–loss effects through the thick target, and finite–geometry effects including kinematic variations, subtraction of accidental coincidences, correction for vertical drift chamber efficiency, and dead–time corrections. The energy correlation for the ^{12}C(p,2p) reaction for the angle pair $\theta_{K600}=14.3°$ and $\theta_c=-64.3°$ is shown in Fig. 1. The diagonal loci represent states of ^{11}B—the residual nucleus. The p_0+^{11}B(g.s.) channel is observed to be the most strongly populated. Summed energy resolution of ≤ 300 keV was obtained for the (p,2p) reaction in this experiment. The resolution obtained for the (p,p′α) data was significantly worse due to energy–loss effects in the thick (2 mg/cm^2) target. The ratio of real to accidental coincidences was greater than 8:1. Events within a given locus are projected onto the horizontal axis yielding that fraction of the proton inelastic scattering yield coincident with the particular charged particle "c". In the following we present results for α and p_0 coincidences.
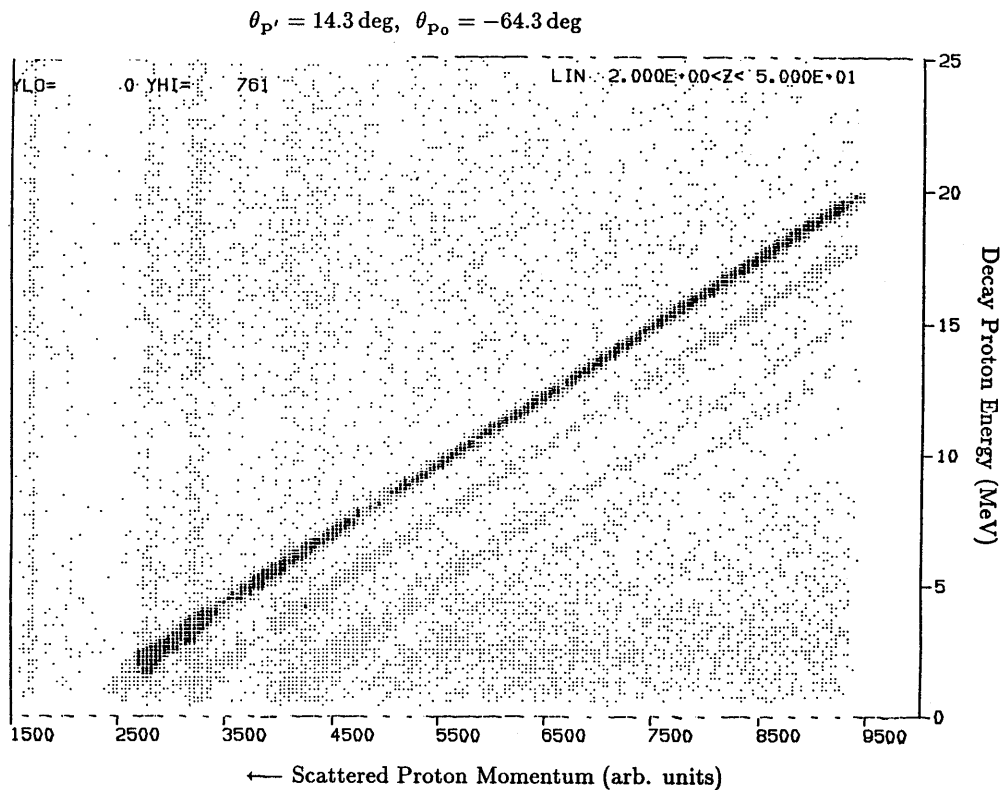

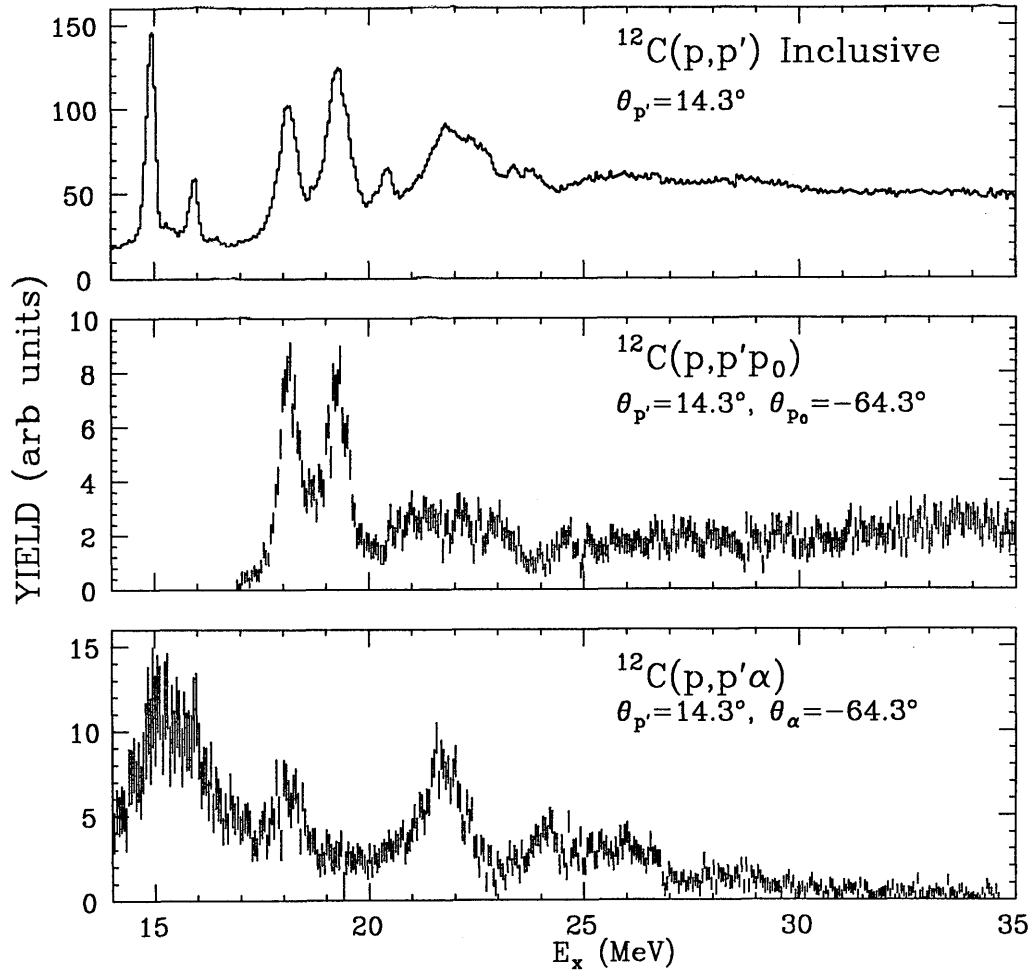Figure 1. Energy correlations for ^{12}C(p,2p) at T$_p$=155.8 MeV, $\theta_{p'}$=14.3°, θ_c=−64.3°.

Figure 2. Comparison of the inclusive, p_0–gated, and α–gated ^{12}C(p,p') spectra at θ_p=14.3° (lab). Coincident particles are detected at θ_c=−64.3° (lab).

Fig. 2 compares the 14.3° inclusive spectrum to the exclusive spectra for coincident p_0 and α particles detected at −64.3°. This correlation angle is essentially parallel to the momentum transfer direction and thus is at nearly 0° in the ^{12}C* rest frame. Below 18 MeV the inclusive spectrum is dominated by the excitation of the broad 2^+,T=0 resonance at 15.4 MeV and the narrow 1^+,T=1 (15.1 MeV) and 2^+,T=1 (16.1 MeV) states. The threshold for proton emission from ^{12}C is at E_x=15.96 MeV. Proton decays from the 16.1 MeV state are not observed due to our detection threshold and use of a thick target. The broad 15.4 MeV resonance is prominent in the (p,p'α) spectrum. The yield from this state is found to be strongly peaked around the momentum transfer direction. At larger correlation angles, significant yields are observed from the 16.1 MeV state. This is consistent with the known large partial width for decay of this state into ^{8}Be(2^+)+α_1.[2] There is only weak evidence for α_1 decay from the 15.1 MeV state, which is again consistent with its known small partial width.[2]

Peaks from the 18.35 MeV $(2^-,T=0)$ and 19.40 MeV $(2^-,T=1)$ states are also prominent in the inclusive yield at small q. The former is observed to have both p_0 and α decays. A detailed examination of the α energy distribution indicates that there is no evidence for α_0 decays; only α_1 decays are necessary to understand the spectrum. This is consistent with the 2^- spin assignment (α_0 decays are forbidden by parity conservation). The similarity of the width and centroid of the 18.35 MeV peak for the α-gated and p_0-gated spectra suggest observation of only a single state even though there is published evidence of more than one state near 18.4 MeV.[2] We find no evidence of yield from the 19.40 MeV state in any of our $(p,p'\alpha)$ spectra which is consistent with the $T=1$ assignment for this state. The p_0 yields have been extracted by peakfitting the exclusive spectrum. No background is necessary to include in the analysis if Lorentzian functions are used for the lineshapes.

Fig. 3 displays the 2^- data compared with angular correlation calculations. The calculations were performed assuming sequential resonance excitation and decay. The exci-
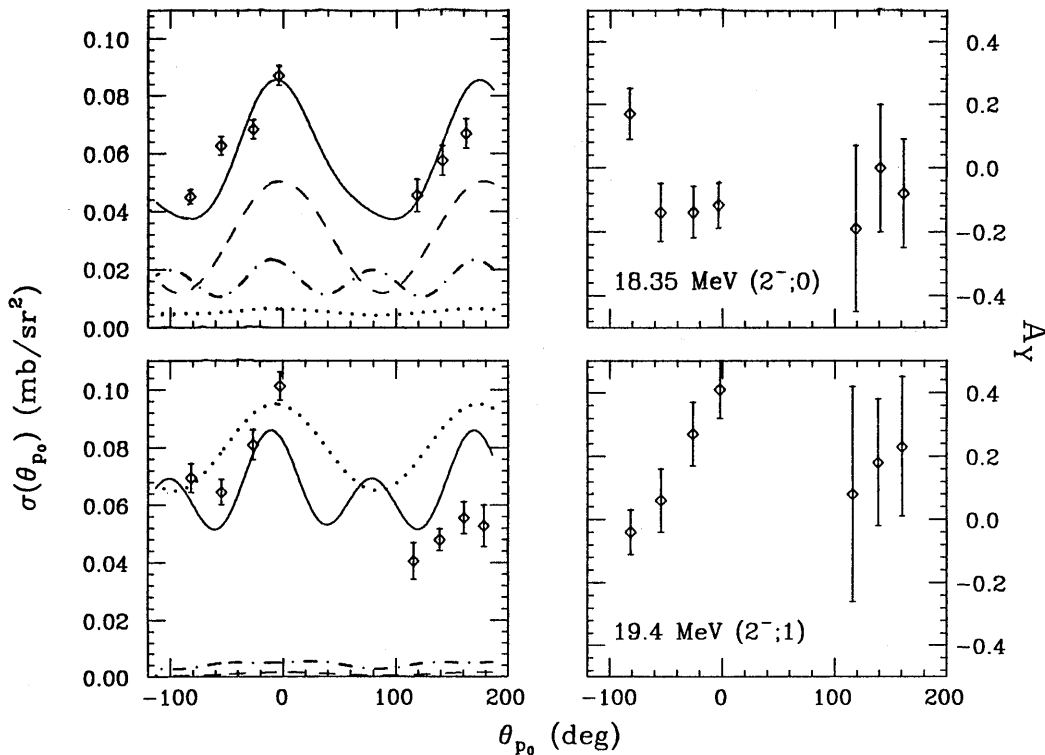

Figure 3. Double–differential cross section and analyzing–power correlations for p_0 decays from the 2^- states at 18.35 and 19.40 MeV. The cross section is plotted against the decay proton polar angle in the $^{12}C^*$ rest frame (with the $\hat{z}$-axis along the (p,p') momentum transfer direction.) Positive angle denotes rotation towards beam left in the scattering plane. The curves are results of DWIA correlation calculations discussed in the text. The different curves represent calculations using the different components of the N-N interaction: solid curve – full interaction; dotted curve – central-spin only; dashed curve – spin-orbit only; and dot-dashed curve – tensor only.

tation was calculated using a standard DWIA code and the Love-Franey nucleon-nucleon interaction.[3] The scattering amplitudes from this calculation were used to compute the density matrix for the $^{12}C^*$ m-states (nuclear spin projections.) The angular correlation function is calculated given this m-state density matrix and assumptions about the orbital angular momentum involved in the decay. The transition density for both states is assumed to be the single particle/hole configuration, $1d_{5/2}1p_{3/2}^{-1}$, coupled to $J^\pi=2^-$. A previous study of proton inelastic scattering cross section and spin observable angular distributions identified this as the dominant configuration for these states.[4] For the angular correlation calculations, we assumed that the p_0 decay is pure d wave from the unbound $1d_{5/2}$ orbital. The branching ratio to the $p_0+^{11}B$ channel was assumed to be 100%. There is good agreement between this calculation and the pattern observed for the 18.35 MeV transition when the calculated correlation function is scaled by 0.6. Inclusion of p_0 decay from the unbound $2s_{1/2}$ orbital would tend to make the correlation function more isotropic (enhancing the agreement.) For the 19.40 MeV state, the data displays a fore/aft asymmetry which the calculation does not reproduce. Furthermore, the data appear more strongly peaked along the momentum transfer direction than does the calculation.

Fig. 3 also shows the sensitivity of the calculated angular correlation function to various parts of the NN interaction used to drive the transition. The T=0 state is observed to result from a constructive interference of amplitudes involving the spin–orbit and tensor interactions. The T=1 state is dominated by the central spin–dependent interaction destructively interfering with small tensor and spin–orbit contributions. The resulting correlation patterns show largest differences in angular ranges which are not easily measured experimentally. Significant differences are observed for the correlation spin–asymmetry function (measured as the incident spin up/down asymmetry as a function of the correlation angle). The simple model described above does not reproduce the features of the correlation spin asymmetry, suggesting that this observable may be sensitive to physics not yet included in the calculation (*e.g.* more complicated transition densities or contributions from other partial waves in the decay.)

Near $E_x=22$ MeV, the inclusive (p,p') spectrum shows a broad bump atop a featureless background. The enhancment has been determined from previous inclusive studies[1] to be the giant dipole resonance (GDR) observed in photoabsorption studies.[5] In the (p,p'p_0) exclusive spectrum, the background observed in the inclusive scattering is greatly reduced, but the peak–to–background ratio is not as improved for the GDR as it was in the case of the 2^- states. The shape of the p_0–gated spectrum in this region of excitation is observed to change as a function of the correlation angle. This behavior may be consistent with correlation–angle dependence of contributions from other $^{12}C^*$ resonances of different J^π. Sizeable fore/aft asymmetries are observed in the correlation functions for all energy bins. These asymmetries are likely due to coherent contributions from the pp quasifree knockout "background" which are peaked at correlation angles near q – *i.e.* forward angles in the $^{12}C^*$ rest frame.

Yields have been extracted by summing the triple–differential cross section in energy bins of 0.5 MeV (Fig. 4). No attempt has been made to subtract an (arbitrary) background. Thus, contributions from quasifree pp scattering are included with those from sequential resonance excitation and decay. Near $E_x=22$ MeV, the angular correlation patterns vary
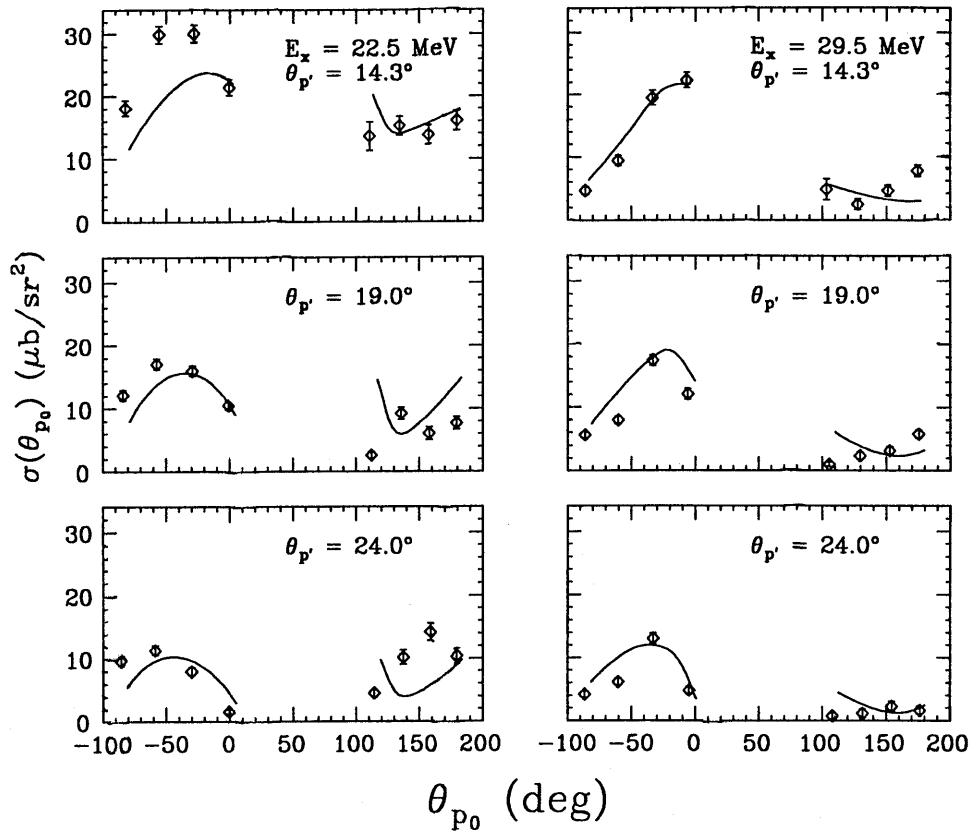
Figure 4. Double–differential cross section correlations for 0.5 MeV wide continuum slices centered at E_x=22.25 and 29.25 MeV. The curves are results of the 3D calculations discussed in the text.

significantly with energy bin and the q dependence of these patterns is large. This behavior is different from the higher excitation energy data ($E_x \geq 25$ MeV) where the correlation function behavior is similar in all excitation energy bins and the q dependence is weak. This provides evidence that the angular correlation data will permit identification of the $\Delta L=1$ yield excited by (p,p′) in the region of the GDR. The higher–excitation data are probably consistent with non–resonant quasifree pp scattering.

A large peak is observed in the (p,p′α) spectrum in the vicinity of the GDR. The angular correlation and q–dependence of the yield from this peak are similar to that observed for the E_x=18.35 MeV state. This is suggestive of dominance of $\Delta L=1$ for the population of the state. The sizeable α decay yield suggests the occurrence of a T=0 intermediate state. A $J^{\pi}=1^-$,T=0 state, nearly degenerate with the GDR in ^{12}C, may explain sizeable differences in the (γ,p$_0$) and (γ,n$_0$) cross sections reported in this region of excitation.[5]

In Fig. 4 we compare our data at higher excitation energies to distorted–wave calculations using the program 3D.[6] In these calculations, the transition density used in the "tρ" prescription for the interaction potential is replaced by the product of the bound–state wave function of the struck nucleon and a wave function describing the relative motion of the unbound system p$_0$+^{11}B. The latter is the solution to the Schrodinger equation using

a complex potential. In general, this potential will have resonant solutions for specific partial waves at certain values of the relative energy. It is these single–particle resonances which are involved in constructing the "giant" resonances observed in the inclusive spectrum. In the calculations presented, the $p_0+^{11}B$ potential has a resonance in the $d_{5/2}$ partial wave at the excitation energy of the GDR. The potential also includes non–zero phase shifts for the other (non–resonant) partial waves. Inclusion of contributions from both resonant and non-resonant partial waves represents the coherent addition of quasifree knockout amplitudes with the amplitude which describes the GDR excitation and decay. In the present model, the latter does not describe decay from a $^{12}C^*$ intermediate state of good J^π and T, rather it is simply a single–particle resonance. The shape of the angular correlation pattern near the resonance and at higher excitation energy is fairly well described by this calculation. The q dependence of the data is also reasonably well described. The calculations all have the same normalization factor (≈ 0.7). The agreement is better for the higher excitation energies and for the more forward (in the $^{12}C^*$ rest frame) decay proton angles, where the intermediate (^{12}C) state structure effects should be diminished relative to the nonresonant scattering. It is anticipated that an improved description of the exclusive yields can be obtained by using a transition density from the continuum shell model.

1. M. Buenerd, P. Martin, P. de Saintignon and J. M. Loiseaux, Nucl. Phys. **A286**, 377 (1977).
2. F. Ajzenberg–Selove, Nucl. Phys. **A433**, 1 (1985).
3. Computer Codes ALLWRLD and TAMURA, F. Petrovich *et al.*, unpublished; M. A. Franey and W. G. Love, Phys. Rev. C **31**, 488 (1985).
4. K. W. Jones, *et al.*, Phys. Lett. **128B**, 281 (1983).
5. M. T. Collins, *et al.*, Phys. Rev. C **26**, 332 (1982).
6. N. S. Chant and P. G. Roos, Phys. Rev. C **15**, 57 (1977). N. S. Chant and P. G. Roos, Phys. Rev. C **27**, 1060 (1983).